ISBN: 978-3-95450-214-1 ISSN: 2673-5490 doi:10.18429/JACoW-IPAC2021-MOPAB054

START-TO-END SIMULATION OF A FREE ELECTRON LASER DRIVEN BY A LASER-PLASMA WAKEFIELD ACCELERATOR*

Weihang Liu[1], Yi Jiao†, Sheng Wang[1]‡
Institute of High Energy Physics, Chinese Academy of Sciences, Beijing 100049, China
University of Chinese Academy of Sciences, Beijing 100049, China
[1]also at Spallation Neutron Source Science Center, Dongguan 523803, China

Abstract

The rapid development of laser-plasma wakefield accelerator (LPA) has opened up a new possible way to achieve ultra-compact free-electron laser (FEL). To this end, LPA experts have made many efforts to generate electron beams with sub-micrometer emittance and low energy spread. Recently, a new laser modulation method was proposed for generating EUV coherent pulse in an LPA-driven FEL. The simulation demonstration of this scheme is based on the Gaussian beam. However, the distribution of the LPA beam is not Gaussian. To further verify the feasibility of the method mentioned above, a start-to-end simulation is required.

INTRODUCTION

The Laser-plasma wakefield accelerator (LPA) driven free-electron laser (FEL) has been widely studied in recent years. Many methods have been proposed to handle the beam divergence and energy spread issue. In particular, a coherent harmonic generation (CHG) method for producing femtosecond coherent radiation in LPA-driven FEL was proposed [1]. This method uses laser energy modulation and transverse-longitudinal coupling beamlines to generate microbunching structures in the LPA beam. The bunching factor for this method is independent of the initial energy spread and the beam divergence, promising high-power coherent radiation. In Ref. [1], this method was demonstrated by simulation with an initial Gaussian electron beam. However, the distribution of the LPA beam is not Gaussian. To further verify the feasibility of this method, we provide a start-to-end simulation. The results show that, as stated in Ref. [1], this method can generate femtosecond coherent radiation with peak power more than 3 orders larger than that without using this method.

METHOD REVIEW

The method used in this paper was first proposed in Ref. [1]. As shown in Fig. 1, in this method, a dogleg is using to induce a coupling between the energy and the transverse position of an electron. After passing the dogleg, the electron interacts with a laser in an undulator called modulator. This interaction will generate an energy modulation in the electron beam. Finally, the downstream dispersion section (DS) converts this energy modulation into strong density modulation. Profit from the transverse-longitudinal coupling induced by the dogleg and DS, under some conditions [Eq. (1)], the bunching factor of this method is only related to the initial beam size of the electron beam. Considering that the LPA beam size is in the micron scale, this method will induce a strong microbunching in the LPA beam.

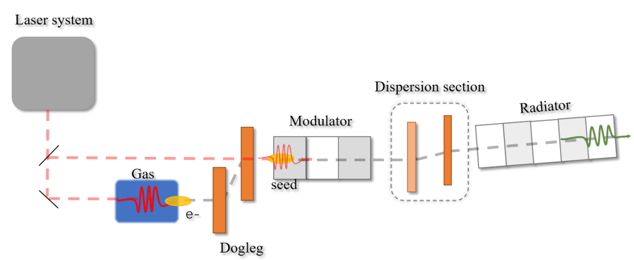

Figure 1: Layout of the CHG method proposed in [1].

The optimization conditions of this method are

$$\begin{cases} \eta_{ds} + (L_m + L_d)\theta_{ds} & = 0, \\ r_{56} - \eta_d \theta_{ds} & = 0, \end{cases} \tag{1}$$

where θ_{ds}, η_{ds} and r_{56} are the $z - x$ coupling term, $z - x'$ coupling term, and longitudinal dispersion of the dispersion section, respectively. L_m is the length of the modulator, η_d and L_d are the dispersion and length of the dogleg, respectively.

When conditions [Eq. (1)] are satisfied, the bunching factor can be expressed in the following form

$$b_n = |J_n(nk_L r_{56}\sigma_\delta A_m)| exp[-\frac{(k_L n)^2}{2}(\theta_{ds}\sigma_{x_0})^2], \tag{2}$$

where k_L is wave number of the laser, A_m is the energy modulation amplitude in the unit of initial energy spread σ_δ. This equation imply that in order to obtain a larger bunching factor, a larger energy modulation amplitude A_m or a larger dispersion η_d is required.

LPA SIMULATION

We adopt the 3D PIC code FBPIC [2] to perform the LPA simulation. To produce a stable, quasi-monoenergetic electron beam, we use the down-ramp injection method [3]. The

* Work supported by National Key Research and Development Program of China (grant No. 2016YFA0401900); Youth Innovation Promotion Association of the Chinese Academy of Sciences (grant No. Y201904); Bureau of Frontier Sciences and Education, Chinese Academy of Sciences (grant No. QYZDJ-SSW-SLH001); National Natural Science Foundation of China (grant No. 11922512).
† jiaoyi@ihep.ac.cn
‡ wangs@ihep.ac.cn

ISBN: 978-3-95450-214-1 ISSN: 2673-5490 doi:10.18429/JACoW-IPAC2021-MOPAB054

profile of the plasma density is shown in Fig. 2. In the down-ramp injection method, the key parameter to control the LPA beam quality is the density gradient. For convenience, we model this density gradient by $\frac{n_1}{n_2}L_{ramp}$, where n_1 and n_2 are the plasma density of the first and second platform, respectively, L_{ramp} is the length of the ramp. Study [4] shows that the shape of the ramp will affect the current profile and the slice emittance, but this effect can be alleviated when the beam charge is high. To simplify, we use a linear ramp (see Fig. 2). In addition, due to the drastic differences in the transverse focusing strength between LPA and traditional magnetic dipole, the beam quality deteriorates [5]. To maintain the beam quality, we adopt a tailored plasma structure with a length of L. With the method shown in Ref. [5], one can match the Twiss parameters between the LPA stage and the laser modulation stage. The corresponding parameters are listed in Table 1.

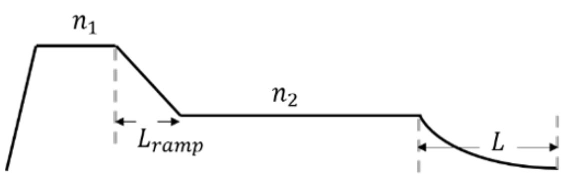

Figure 2: Profile of the plasma density.

Table 1: Parameters of the Plasma and the Driven Laser

Plasma parameters	**Value**	**Unit**
n_1	6×10^{18}	cm^{-3}
Length of the first platform	24.5	µm
L_{ramp}	28	µm
n_2	2.2×10^{18}	cm^{-3}
Length of the second platform	1	mm
L	1.8	mm
Laser parameters		
Wavelength	800	nm
Duration	3.8	µm
Waist size	7.76	µm
Power	37	TW

The final distribution of the LPA beam is shown in Fig. 3, which is not Gaussian. The electron beam energy and RMS energy spread are about 205 MeV and 5.4%, respectively. The slice parameters of the LPA beam are varying along the bunch. As shown in the dotted box of Fig. 3 (c) and (d), due to the beam loading effect [6], there is a region where the slice parameters smoothly change along the bunch. This region is more preferred by the CHG method. The LPA beam parameters are listed in Table 2.

COHERENT HARMONIC GENERATION

The data generated from FBPIC is used by Elegant (with third-order transport effect) and Genesis to simulate the modulation and radiation process.

Before determining the optimization parameters of the CHG method, we need to consider the following two conditions:

- Due to the large beam divergence (0.5 mrad), the undulator parameter K of the modulator should be large enough so that the amplitude of the wiggler motion $K/\gamma \gg \sigma_{x'_0}$.
- The dispersion section needs to be compact enough to ensure that the second-order terms of the transport matrix (T_{522} and T_{544}) have a small effect on the bunching factor.

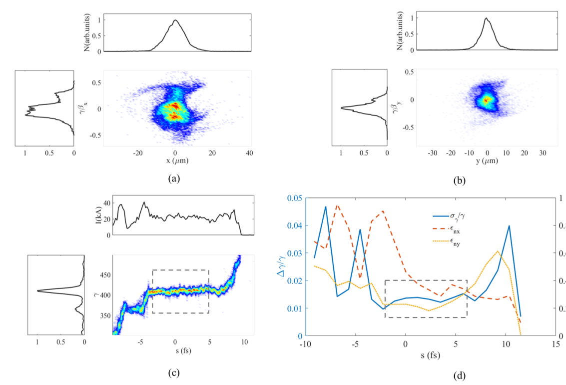

Figure 3: Phase space and beam distribution of the LPA beam in the horizontal (a), vertical (b) and longitudinal direction (c). And the slice parameters for different time slices (d).

Table 2: LPA Beam Parameters

Beam parameters	**Value**	**Unit**
Beam energy	205	MeV
Energy spread (rms/slice)	5.4/1.5	%
Norm. Emittance (rms/slice)	0.8/0.2	µm
Beam size (rms)	6.3	µm
Bunch length (rms)	1.86	µm
Charge	0.35	nC

The parameters of the modulation beamline are listed in Table 3. The phase space after the DS is shown in Fig. 4, which clearly shows that many micro-bunches are generated in the LPA beam.

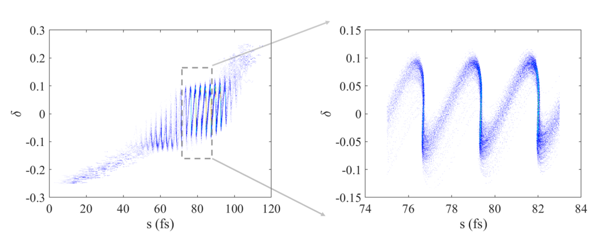

Figure 4: Phase space of the LPA beam after the DS.

ISBN: 978-3-95450-214-1 ISSN: 2673-5490 doi:10.18429/JACoW-IPAC2021-MOPAB054

Table 3: Parameters of the Seed Laser, Beamline and the Radiator

Seed laser	**Value**	**Unit**
Wavelength	800	nm
Ralylength	0.98	m
Peak power	1.4	TW
FWHM duration	10	fs
Dogleg		
Bending angle	14.3	mrad
Bend length	0.15	m
Drift length	0.2	m
Dispersion section		
Bending angle for first dipole	−13.8	mrad
Bend length	0.08	m
Drift between first and second dipoles	0.144	m
Bending angle for second dipole	18.68	mrad
Bend length	0.08	m
Radiator		
Period	1	cm
Period number	16	

The distribution of the bunching factor with a harmonic number of 16 along the bunch is shown in Fig. 5. Due to the nonlinear effects of the DS, the bunching factor is reduced by about 24%. The maximum bunching factor is about 14.7%. This modulated beam is then sent to the downstream undulator with a period length of 1 cm, and a total length of 16 cm for the generation of coherent radiation pulse. The output of the radiation is shown in Fig. 6. The peak power of the radiation pulse is about 70MW, and the RMS bandwidth is about 0.75%.

For comparison, we also simulate the case without using the CHG method. The spontaneous emission (SE) signal is shown in Fig. 7. In this case, the radiation power is three orders lower than that of the CHG, and the bandwidth is one order longer.

Besides, the CHG output with the initial Gaussian beam is also simulated. As shown in Fig. 6 (blue lines), the radiation power of the case using Gaussian beam is slightly higher than that of the case with LPA beam, and the bandwidth is slightly shorter. If one neglect those fine distinction, then for preliminary study, Gaussian beam is a good approximation.

CONCLUSION

In this paper, we perform a start-to-end simulation of an LPA-driven FEL. This LPA-driven FEL is based on a method proposed in Ref. [1]. The results from the start-to-end simulation further verify the feasibility of this method.

ACKNOWLEDGEMENTS

We thank Dr. Dazhang Li, Dr. Ming Zeng, and Dr. Yuhui Li for useful discussion and comments.

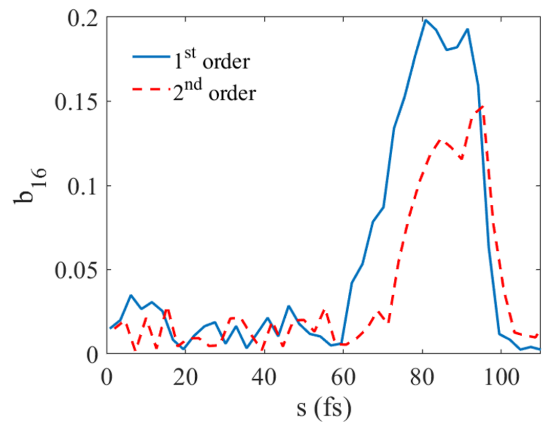

Figure 5: Distribution of the bunching factor with a harmonic number of 16 along the bunch.

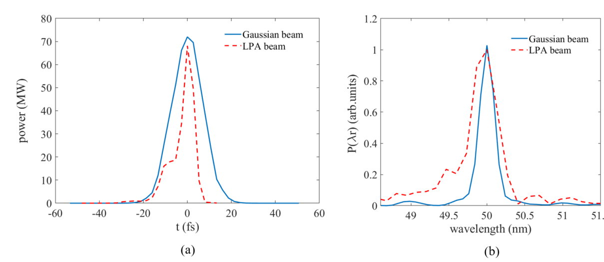

Figure 6: Power distribution (a) and spectrum (b) of the CHG pulse.

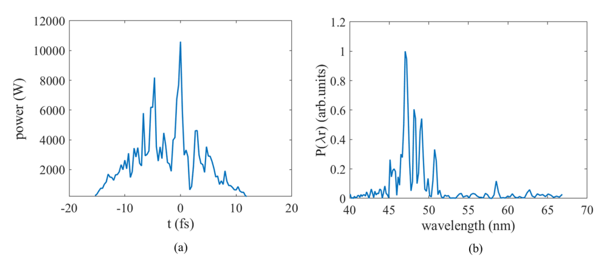

Figure 7: Power distribution (a) and spectrum (b) of the SE pulse.

REFERENCES

[1] W. Liu *et al.*, "A coherent harmonic generation method for producing femtosecond coherent radiation in a laser plasma accelerator based light source", *J. Synchrotron Radiat.*, vol. 28, no. 3, pp. 669–680, Mar. 2021. doi:10.1107/s1600577521002745

[2] M. Kirchen *et al.*, "FBPIC: A spectral, quasi-3D, multi-GPU Particle-In-Cell code for plasma accelerators", *Verhandlungen der Deutschen Physikalischen Gesellschaft*, vol. 50, no. 10, 2018.

[3] S. Bulanov*et al.*, "Particle injection into the wave acceleration phase due to nonlinear wake wave breaking", *Phys. Review E*, vol. 58, no. 5, pp. R5257–R5260, Nov. 1998. doi:10.1103/physreve.58.r5257

ISBN: 978-3-95450-214-1 ISSN: 2673-5490 doi:10.18429/JACoW-IPAC2021-MOPAB054

[4] C. Zhang *et al.*, “Effect of fluctuations in the down ramp plasma source profile on the emittance and current profile of the self-injected beam in a plasma wakefield accelerator”, *Phys. Rev. Accel. Beams*, vol. 22, no. 11, p. 111301, Nov. 2019. doi:10.1103/physrevaccelbeams.22.111301

[5] XL. Xu *et al.*, “Physics of Phase Space Matching for Staging Plasma and Traditional Accelerator Components Using Longitudinally Tailored Plasma Profiles”, *Phys. Rev. Lett.*, vol. 116, no. 12, p.124801, Mar. 2016. doi:10.1103/physrevlett.116.124801

[6] T. Katsouleas *et al.*, “Beam loading in plasma accelerators”, *Particle Accelerators*, vol. 22, pp. 81–99, 1987.